FACTA UNIVERSITATIS
Series: **Mechanical Engineering** Vol. 23, No 4, 2025, pp. 787 - 806
https://doi.org/10.22190/FUME250525028H

Original scientific paper

A FAST INSIGHT INTO HIGH-ACCURACY NONLINEAR FREQUENCY ESTIMATION OF STRINGER-STIFFENED SHELLS

Chun-Hui He[1], Mostafa Mohammadian[2]

[1]School of Civil Engineering and Transportation, Foshan University, Foshan, China
[2]Mechanical Engineering Department, Esfarayen University of Technology, Esfarayen, North Khorasan, Iran

ORCID iDs: Chun-Hui He https://orcid.org/0000-0003-0810-5248
Mostafa Mohammadian http://orcid.org/0000-0002-0714-2787

Abstract. *Understanding the behavior of nonlinear vibrations in stringer-stiffened shell structures is crucial for enhancing the stability and efficiency of advanced aerospace and marine systems. These systems often exhibit complex responses due to geometric and material intricacies, which require analytical methods capable of effectively capturing critical dynamics. This study presents three efficient analytical methods for deriving closed-form expressions for the nonlinear frequency of such systems: the adaptive location point-based He's formulation (ALPF), the square error minimizing-based frequency formulation (SEMF), and the Hamiltonian-based frequency-amplitude formulation (HFAF). These methods offer efficient and straightforward solutions for analyzing nonlinear oscillators without requiring complex iterative procedures. The nonlinear frequency of the stringer-stiffened shell is determined using each method and validated against both exact analytical solutions and numerical results. The results show that the first two methods yield high accuracy for small amplitudes, while their accuracy decreases at higher amplitudes. In contrast, the Hamiltonian-based method maintains high accuracy over a wider range of amplitudes. The original He's formulation is recognized for its simplicity and computational efficiency, making it a practical tool for rapid frequency estimation in stringer-stiffened shell systems. This comparative study offers guidance for selecting appropriate analytical tools for nonlinear vibration analysis of complex mechanical and physical systems.*

Key words: *Stringer-stiffened shell, Approximate analytical solution, Nonlinear frequency, Frequency-amplitude formulation, Nonlinear vibration*

Received: May 25, 2025 / Accepted July 23, 2025
Corresponding author: Mostafa Mohammadian
Mechanical Engineering Department, Esfarayen University of Technology, Azadegan Boulevard, Corner of Mader Square, Esfarayen, North Khorasan, Iran, Postal Code: 9661998195.
E-mail: mo.mohammadyan@gmail.com, mo.mohammadyan@esfarayen.ac.ir.

1. INTRODUCTION

The nonlinear vibration behavior of cylindrical shells constitutes a critical topic in civil and mechanical engineering. The importance of nonlinear vibrations has grown due to their impact across various fields, including physical sciences, engineering, and mechanical systems. Consequently, engineering design processes are increasingly focused on the dynamic behavior of beams and shells. In particular, the nonlinear vibration of cylindrical shells plays a vital role in mechanical engineering, especially in aerospace and marine applications. Stringer-stiffened shells play a foundational role in the design of aircraft, spacecraft, and ships, which are frequently subjected to dynamic loading conditions. A deeper understanding of their nonlinear response can significantly enhance performance and structural integrity. This study aims to address the need for efficient and accurate methods to predict the nonlinear frequency of stringer-stiffened shells. Such methods are essential for improving structural safety and reliability in engineering applications.

The dynamic behavior and stability of shell structures have been thoroughly studied due to their critical role in modern engineering applications. Gavrilenko and Matsner [1] examined the buckling characteristics of stringer shells, highlighting the influence of stiffening elements on structural stability. Naghsh et al. [2] utilized a meridional finite strip method to analyze free vibrations of various shell structures. Golchi et al. [3] explored thermal buckling and free vibration of functionally graded (FG) truncated conical shells with stringer and ring stiffeners. Bich and Ninh [4] pioneered this area by investigating nonlinear vibrations in imperfect stiffened sandwich toroidal shells under thermo-mechanical loading. They later extended their work [5] to eccentrically stiffened toroidal shell segments on elastic foundations. Recent research by Liu et al. [6] focused on nonlinear traveling-wave vibrations of ring-stringer stiffened cylindrical shells, highlighting the complexity introduced by wave propagation. A significant body of research has been dedicated to the exploration of rotational and thermal effects on the shell's nonlinear dynamics. Liu et al. [7] analyzed nonlinear forced vibrations in rotating cylindrical shells under multi-harmonic excitations in thermal environments. Vahidi et al. [8] investigated the nonlinear vibration, stability, and bifurcation of rotating axially moving conical shells, providing insight into the dynamic instabilities induced by axial motion and rotation. Mohammadrezazadeh and Jafari [9] proposed vibration suppression in laminated composite cylindrical shells employing magneto strictive strips. Recent advancements include high-fidelity modeling and simulation techniques for stiffened cylindrical shells under various loading scenarios. Bochkarev et al. [10] studied panel flutter in stiffened shallow shell structures. Foroutan and Dai [11] investigated nonlinear dynamics in spiral-stiffened FG toroidal shells with variable thickness. Azzara et al. [12] analyzed rotor dynamic responses of stiffened cylindrical structures using high-order shell models. Zhang et al. [13] explored frequency responses in porous hyperplastic Mooney-Rivlin cylindrical shells under radial harmonic forces. Du et al. [14] developed a semi-analytical method for the vibration control in cylindrical shell structures. Chen et al. [15] examined the correlation between welding parameters and vibro-acoustic behavior in stiffened cylindrical shells. Tan et al. [16] introduced innovative sandwich composite shell structures and established a framework for nonlinear geometric and dynamic analyses. Khoddami Maraghi et al. [17] investigated free vibrations of truncated conical sandwich shells with auxetic core and polymeric nanocomposite face sheets reinforced with graphene nanoplatelets. Despite substantial progress, further research is needed to account for multi-physical interactions, enhance model accuracy, and develop efficient computational techniques for design and optimization.

Solution methods for nonlinear differential equations are typically categorized into numerical and analytical approaches. The free vibration and stability of stringer-stiffened shells have been the subject of various numerical investigations [2, 18, 19]. In this context, developments in finite element methods for laminated shell structures [20], as well as in isogeometric finite element formulations [21], have provided highly efficient numerical tools relevant to such analyses. However, solving nonlinear problems with high accuracy presents a considerable challenge, and obtaining exact analytical solutions is often even more complex. To overcome these limitations, researchers have developed several advanced approximate analytical techniques. These methods include the harmonic balance method (HBM) [22, 23], the energy balance method (EBM) [24, 25], the homotopy perturbation method (HPM) [26], the Li–He's modified homotopy perturbation method (LI-HE HPM) [27], the Hamiltonian approach (HA) [28, 29], the variational iteration algorithms (VIM) [30, 31], the global error minimization (GEM) [32, 33], the modified algebraic method (MAM) [34, 35], and the variational approach (VA) [36]. In recent studies, the HA [37], the HPM [38], and the global residue harmonic balance method (GRHBM) [39] have been employed to determine the nonlinear frequency of stringer-stiffened shells. Despite their effectiveness, each method has notable limitations when applied to complex geometries like stringer-stiffened shells. The HA often requires complex energy formulations and extensive algebraic manipulation, making it computationally demanding and less suitable for systems involving damping or external forces. The HPM, despite its flexibility, relies on iterative series expansions and the construction of a suitable homotopy. This process can be arduous and time-consuming for higher-order nonlinear systems. Furthermore, the accuracy of the model tends to decrease at large amplitudes. The GRHBM is recognized for its precision; however, it requires balancing multiple harmonics and computing global residuals, which leads to high algebraic complexity and necessitates the use of symbolic computation tools.

Despite significant progress in the field, existing analytical methodologies continue to face challenges in balancing simplicity, accuracy, and applicability to the strongly nonlinear dynamics of stringer-stiffened shells, particularly at large vibration amplitudes. The cubic-quintic nonlinearities resulting from geometric and material effects demand rapid, non-iterative solutions that retain accuracy across a wide amplitude range. This study proposes three novel analytical methods: the Adaptive Location Point-based He's Formulation (ALPF), the Square Error Minimizing-based Frequency Formulation (SEMF), and the Hamiltonian-based Frequency-Amplitude Formulation (HFAF), to derive closed-form expressions for the nonlinear frequency of stringer-stiffened shells. These approaches are optimized for simplicity and computational efficiency, effectively overcoming the complexity of earlier methods while maintaining high accuracy. Their performance is validated through comparisons with exact solutions and numerical simulations. The proposed methods offer practical tools for engineers and researchers studying nonlinear vibrations in complex shell structures.

2. Mathematical Model

As illustrated in Fig. 1, a circular cylindrical shell is stiffened by uniformly distributed external stringers. The supports consist of ribs, modeled as one-dimensional elastic elements, which are evenly spaced along the shell. To determine the displacements and vibration frequencies, it is assumed that rib height is much smaller than the shell's radius of curvature. Moreover, interaction between the ribs in the two directions is neglected.

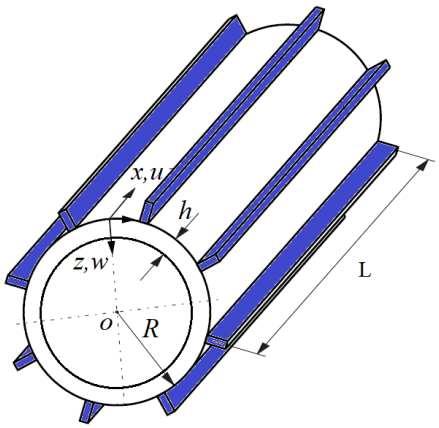

Fig. 1 A schematic view of a stringer-stiffened shell structure

To study the dynamics of the orthotropic stringer-stiffened shell under large displacements, the following governing equations are employed [40]:

$$\nabla_1^4 w - R\frac{\partial^2 \varphi}{\partial x^2} + \rho R^2 \frac{\partial^2 w}{\partial t^2} - L(w,\varphi) = 0, \tag{1}$$

$$\frac{1}{B_1}\frac{\partial^4 \varphi}{\partial y^4} + \frac{1}{R}\frac{\partial^4 w}{\partial x^2} - \frac{1}{2R^2}L(w,\varphi) = 0, \tag{2}$$

where

$$\nabla_1^4 w = \frac{1}{R^2}\left(D_1\frac{\partial^4}{\partial x^4} + 2D_3\frac{\partial^4}{\partial x^2 \partial y^2} + D_2\frac{\partial^4}{\partial y^4}\right), \tag{3}$$

$$L(w,\varphi) = \left(\frac{\partial^2 w}{\partial x^2}\frac{\partial^2 \varphi}{\partial y^2} - 2\frac{\partial^2 w}{\partial x \partial y}\frac{\partial^2 \varphi}{\partial x \partial y} + \frac{\partial^2 \varphi}{\partial x^2}\frac{\partial^2 w}{\partial y^2}\right), \tag{4}$$

$$\rho = \rho_0 h + \frac{N\rho_1 F}{2\pi R}, \qquad B_1 = \frac{NE_1 F}{2\pi R} + \frac{Eh}{1-\upsilon^2}, \tag{5}$$

in which, w and φ denote the lateral displacement and the Airy stress function, respectively. R represents the shell radius, and h is its thickness. ρ_0 and ρ_1 are the densities of the shell and stringer materials, respectively. N denotes the number of stringers, and F is the cross-sectional area of a stringer. E and E_1 represent the elastic modulus of the shell and stringer materials, respectively. Additionally, υ denotes Poisson's ratio. The coefficients D_i (i = 1, 2, 3) are material-dependent parameters associated with the stiffened shell, as reported in [41]. For simply supported boundary conditions (SS BCs), the displacement w can be approximated as follows [38]:

$$w(x,y,t) = f_1(t)\sin\left(\frac{m\pi}{L}x\right)\cos(ny) + \frac{f_1^2(t)n^2}{4R}\sin^2\left(\frac{m\pi}{L}x\right), \tag{6}$$

where m and n denote the wave numbers in the axial and circumferential directions, respectively. Using Eqs. (1) and (6), the Airy function is obtained as follows:

$$\begin{aligned} B_1^{-1}\varphi = {} & \frac{m^2\pi^2}{n^4L^2}\frac{f_1}{R}\sin\left(\frac{m\pi}{L}x\right)\cos(ny) - \frac{5}{16}\left(\frac{m_1}{n_1}\right)^2\frac{f_1^2}{R^2}\cos(2ny) \\ & + \frac{1}{2}\frac{m^2\pi^2}{L^2}\frac{f_1^3}{R^3}\sin\left(\frac{m\pi}{L}x\right)\cos\left(\frac{2m\pi}{L}x\right)\cos(ny). \end{aligned} \tag{7}$$

By considering $u(t) = f_1(t)/R$ and applying the Galerkin method, the governing differential equation for the dynamics of the stringer-stiffened shell is derived as:

$$\frac{d^2u}{dt^2} + \beta_1\left(u^2\frac{d^2u}{dt^2} + u\left(\frac{du}{dt}\right)^2\right) + \beta_2 u + \beta_3 u^3 + \beta_4 u^5 = 0, \tag{8}$$

where the coefficients β_i (i = 1, 2, 3, 4) are defined as follows:

$$\begin{aligned} & \beta_1 = 0.09375n^4, \beta_2 = \varepsilon_1^2\varepsilon_4 + 2\varepsilon_1^2\varepsilon_4\varepsilon_3\frac{n^2L^2}{\pi^2m^2} + \varepsilon_1^2\varepsilon_4\varepsilon_2\frac{n^4L^4}{\pi^4m^4} + \frac{1}{n^4}\left(1-\varepsilon_6^2n^2\right)^2, \\ & \beta_3 = 0.0625 + 0.5n^4\varepsilon_1^2\varepsilon_4 - 0.75\left(1-\varepsilon_6^2n^2\right), \beta_4 = 0.25n^4, \end{aligned} \tag{9}$$

and the coefficients ε_i (i = 1, 2, …6) are defined in [41]. For doubly clamped boundary conditions (CC BCs), the displacement w can be approximated as follows:

$$w(x,y,t) = f_1(t)\sin^2\left(\frac{m\pi}{L}x\right)\cos(ny) + \frac{3f_1^2(t)n^2}{16R}\sin^2\left(\frac{m\pi}{L}x\right). \tag{10}$$

Following the outlined procedure, the values β_i for CC BCs are determined as follows:

$$\begin{aligned} & \beta_1 = 0.140625n^4, \beta_3 = 0.083 + 0.1875n^4\varepsilon_1^2\varepsilon_4 - 1.5\left(1-\varepsilon_6^2n^2\right), \beta_4 = 0.1641n^4, \\ & \beta_2 = 5.33\varepsilon_1^2\varepsilon_4 + 2.67\varepsilon_1^2\varepsilon_4\varepsilon_3\frac{n^2L^2}{\pi^2m^2} + \varepsilon_1^2\varepsilon_2\frac{n^4L^4}{\pi^4m^4} + 5.33\frac{1}{n^4}\left(1-\varepsilon_6^2n^2\right)^2, \end{aligned} \tag{11}$$

where the coefficients ε_i (i = 1, 2, …6) can be found in [41]. The governing nonlinear differential equation presented in Eq. (8) is highly nonlinear due to the presence of cubic-quintic nonlinear restoring force terms, as well as displacement-dependent dynamic terms such as $u^2\ddot{u}$ and $u\dot{u}^2$. These terms introduce a strong amplitude dependence into the system's response, further complicating the governing equation. In the following section, approximate analytical solutions are derived for Eq. (8), considering the initial conditions:

$$u(0) = A, \quad \left.\frac{du}{dt}\right|_{t=0} = 0. \tag{12}$$

Although Eq. (8) is specifically derived for a stringer-stiffened shell structure, it also represents the governing dynamic differential equation of other structural systems. For example, by setting $\beta_4 = 0$, the equation reduces to the form encountered in tapered beams [42]. Similarly, setting $\beta_1 = 0$ yields the well-known Duffing equation, which is widely used in engineering and physics applications, such as modeling undamped FG beams [43]. Therefore, the analytical methods proposed herein are not limited to the specific geometry considered but can be more broadly applied to estimate the nonlinear frequency of a wide range of conservative systems.

3. Analytical Solutions for Nonlinear Vibration of the Stringer-Stiffened Shell

This section derives closed-form expressions for the nonlinear frequency of the stringer-stiffened shell governed in Eq. (8), by proposing three straightforward and non-iterative approximate analytical methods. For validation purpose, the exact nonlinear frequency is also derived. Each method assumes a trial solution of the form $u(t) = A\cos(\omega t)$, which satisfies the initial conditions specified in Eq. (12) and approximates the periodic behavior of the oscillator.

3.1. Adaptive Location Point-based He's Formulation (ALPF)

In this paper, we propose a new method, namely the adaptive location point-based He's formulation (ALPF), to improve He's frequency–amplitude formulation. In the original method, a fixed location point is selected based on He's recommendation. In contrast, ALPF introduces a procedure for selecting the location point, according to the system's amplitude and physical parameters. This adaptation improves the accuracy of the estimated frequency, especially in systems with strong nonlinearities or amplitude-dependent behavior. Importantly, ALPF retains the simplicity and computational efficiency of the original method. To illustrate the method, consider the differential equation of a nonlinear oscillator given by:

$$\ddot{u} + F(u) = 0, \quad u(0) = A, \quad \dot{u}(0) = 0. \tag{13}$$

The above equation can be rewritten as

$$\ddot{u} + \left(\frac{F(u)}{u}\right)u = 0. \tag{14}$$

He [44, 45] demonstrated that the frequency of the nonlinear oscillator given in Eq. (13) can be easily approximated as follows:

$$\omega_{He}^2 \approx \left.\frac{F(u)}{u}\right|_{u=\bar{u}}, \tag{15}$$

where $\bar{u}$ is the location point, defined as $\bar{u} = kA$. This formulation has been widely applied to various types of nonlinear oscillators. The method is computationally simple, making it suitable for quick frequency estimations. However, one of the main challenges in applying He's method is selecting an appropriate value for the location point [27]. It is more

appropriate to express the value of k as a function of both the amplitude and system parameters. To implement the proposed ALPF method, Eq. (15) is substituted into Eq. (13), allowing the latter to be rewritten in the following form:

$$\ddot{u} + g(kA)u = g(kA)u - F(u), \qquad g(kA) = \left.\frac{F(u)}{u}\right|_{u=kA}. \tag{16}$$

If the frequency obtained from Eq. (15) is regarded as the exact frequency, then the right-hand side of Eq. (16) reduces to zero. By applying the Galerkin technique and using $\cos(\omega t)$ as the weighting function, the following equation is derived:

$$\int_0^{T/4} \left(g(kA)u - F(u)\right)\cos(\omega t)dt = 0, \tag{17}$$

where $T = 2\pi/\omega$. This equation can be solved to determine the value of k. For the present problem, Eq. (8) can be rewritten as:

$$\ddot{u} + \left(\frac{\beta_1\left(u^2\ddot{u} + u\dot{u}^2\right) + \beta_2 u + \beta_3 u^3 + \beta_4 u^5}{u}\right)u = 0. \tag{18}$$

Following Eq. (15), the nonlinear frequency is approximated as:

$$\omega_{He}^2 = \left.\frac{\beta_1\left(u^2\ddot{u} + u\dot{u}^2\right) + \beta_2 u + \beta_3 u^3 + \beta_4 u^5}{u}\right|_{u=\bar{u},\dot{u}=\bar{\dot{u}},\ddot{u}=\bar{\ddot{u}}}. \tag{19}$$

When $\bar{u} = kA$, we have $\bar{\dot{u}} = -A\omega\sqrt{1-k^2}$, and $\bar{\ddot{u}} = -kA\omega^2$. Substituting these values into Eq. (19) yields the approximate nonlinear frequency as follows:

$$\omega_{He} = \sqrt{\frac{\beta_2 + \beta_3 k^2 A^2 + \beta_4 k^4 A^4}{1 + 2\beta_1 k^2 A^2 - \beta_1 A^2}}, \tag{20}$$

and the approximate solution as:

$$u_{He}(t) = A\cos\left(\sqrt{\frac{\beta_2 + \beta_3 k^2 A^2 + \beta_4 k^4 A^4}{1 + 2\beta_1 k^2 A^2 - \beta_1 A^2}}\,t\right). \tag{21}$$

Using the specific value $k = \sqrt{3}/2$ recommended in [46], the approximate nonlinear frequency can be expressed as follows:

$$\omega_{He} = \sqrt{\frac{16\beta_2 + 12\beta_3 A^2 + 9\beta_4 A^4}{16 + 8\beta_1 A^2}}. \tag{22}$$

To obtain a more accurate frequency, Eq. (8) is reformulated using the proposed ALPF approach as follows:

$$\frac{d^2u}{dt^2}+\left(\frac{\beta_2+\beta_3k^2A^2+\beta_4k^4A^4}{1+2\beta_1k^2A^2-\beta_1A^2}\right)u= \\ \left(\frac{\beta_2+\beta_3k^2A^2+\beta_4k^4A^4}{1+2\beta_1k^2A^2-\beta_1A^2}\right)u-\beta_1\left(u^2\frac{d^2u}{dt^2}+u\left(\frac{du}{dt}\right)^2\right)-\beta_2u-\beta_3u^3-\beta_4u^5. \tag{23}$$

If the frequency obtained from Eq. (18) is the exact frequency, then the right-hand side of Eq. (23) becomes zero. Based on Eq. (17), we obtain:

$$\int_0^{T/4}\left(\frac{\beta_2+\beta_3k^2A^2+\beta_4k^4A^4}{1+2\beta_1k^2A^2-\beta_1A^2}u-\beta_1\left(u^2\frac{d^2u}{dt^2}+u\left(\frac{du}{dt}\right)^2\right)-\beta_2u-\beta_3u^3-\beta_4u^5\right)\cos(\omega t)dt=0. \tag{24}$$

Substituting Eq. (21) into Eq. (24) and solving the resulting equation yields the following expression for k:

$$k=\sqrt{\frac{-\Gamma_2+\sqrt{\Gamma_2^2-4\Gamma_1\Gamma_3}}{2\Gamma_1}}, \tag{25}$$

where

$$\Gamma_1=8\beta_4A^2+4\beta_4\beta_1A^4,\quad \Gamma_2=-10\beta_4\beta_1A^4+8\beta_3-16\beta_1\beta_2-8\beta_3\beta_1A^2, \\ \Gamma_3=5\beta_4\beta_1A^4-6\beta_3+12\beta_1\beta_2+6\beta_3\beta_1A^2-5\beta_4A^2. \tag{26}$$

Eq. (25) provides an appropriate location point that depends on both the amplitude and the system parameters. By substituting the value of k, calculated from Eq. (25), into Eq. (20), the approximate frequency denoted as ω_{ALPF} is determined using the proposed ALPF method.

3.2. Square Error Minimizing-based Frequency Formulation (SEMF)

The square error minimizing-based frequency formulation (SEMF), proposed in [47], is a mathematical refinement of He's frequency formulation. It provides a modified approach that enhances the accuracy of the approximate frequency by minimizing a square error function. The error function $E(\omega^2)$, corresponding to Eq. (13), is defined as follows:

$$E(\omega^2)=\left|F(u)-\omega^2(A)u(t)\right|. \tag{27}$$

We define the mean square error as follows:

$$\bar{E}^2(\omega^2)=\int_0^{T/4}\left(F(u)-\omega^2(A)u(t)\right)^2dt. \tag{28}$$

To minimize the error, it is required that

$$\frac{d\bar{E}^2(\omega^2)}{d(\omega^2)}=\frac{d}{d(\omega^2)}\int_0^{T/4}\left(F^2(u)-2\omega^2(A)u(t)F(u)+\omega^4(A)u^2(t)\right)dt=0. \tag{29}$$

By solving Eq. (29), an approximate expression for the nonlinear oscillator frequency given in Eq. (13) is obtained as [47]:

$$\omega_{SEMF}^2 = \frac{\int_0^{T/4} u(t)F(u)dt}{\int_0^{T/4} u^2(t)dt}. \tag{30}$$

For the present problem, Eq (30) can be formulated as follows

$$\omega_{SEMF}^2 = \frac{\int_0^{T/4} u(t)\left(\beta_1\left(u^2\ddot{u}+u\dot{u}^2\right)+\beta_2 u+\beta_3 u^3+\beta_4 u^5\right)dt}{\int_0^{T/4} u^2(t)dt}. \tag{31}$$

By substituting $u(t)=A\cos(\omega t)$ into Eq. (31), the following expression is obtained:

$$\begin{aligned}\omega_{SEMF}^2 = &\frac{\int_0^{T/4} \beta_1 A\cos(\omega t)\left(-A^3\omega^2\cos^3(\omega t)+A^3\omega^2\cos(\omega t)\sin^2(\omega t)\right)dt}{\int_0^{T/4} A^2\cos^2(\omega t)dt}\\ &+\frac{\int_0^{T/4} A\cos(\omega t)\left(\beta_2 A\cos(\omega t)+\beta_3 A^3\cos^3(\omega t)+\beta_4 A^5\cos^5(\omega t)\right)dt}{\int_0^{T/4} A^2\cos^2(\omega t)dt}.\end{aligned} \tag{32}$$

After simplification, the expression for the nonlinear frequency of the stringer-stiffened shell can be written as:

$$\omega_{SEMF} = \sqrt{\frac{16\beta_2+12\beta_3A^2+10\beta_4A^4}{16+8\beta_1A^2}}, \tag{33}$$

and the approximate solution as

$$u_{SEMF}(t) = A\cos\left(\sqrt{\frac{16\beta_2+12\beta_3A^2+10\beta_4A^4}{16+8\beta_1A^2}}t\right). \tag{34}$$

This method achieves a balance between accuracy and simplicity by optimizing the error and demonstrates robustness for amplitudes ranging from small to moderate. It should be noted that the frequency derived in Eq. (33) can also be obtained using the HA [37], the HPM [38], and the first-order GRHBM [39].

3.3. Hamiltonian-based Frequency-Amplitude Formulation (HFAF)

The Hamiltonian-based method [48] utilizes energy conservation to estimate the frequency. For the nonlinear oscillator given in Eq. (13), the Hamiltonian constant H is defined as follows:

$$H = \frac{1}{2}\left(\frac{du}{dt}\right)^2 + P(u), \tag{35}$$

where $P(u) = \int F(u)du$. For a conservative system, the Hamiltonian remains constant during the entire oscillation process. Therefore, we have:

$$\frac{1}{2}\left(\frac{du}{dt}\right)^2 + P(u) - P(A) = 0. \tag{36}$$

By substituting the approximate solution $u(t)=A\cos(\omega t)$ into Eq. (36), the corresponding residual function is obtained as follows:

$$R(t) = \frac{1}{2}A^2\omega^2 \sin^2(\omega t) + P\left(A\cos(\omega t)\right) - P\left(A\right). \tag{37}$$

By defining two average residuals

$$\bar{R}_1 = \frac{4}{T_1}\int_0^{T_1/4} R_1 \cos(\omega_1 t)dt, \tag{38}$$

$$\bar{R}_2 = \frac{4}{T_2}\int_0^{T_2/4} R_2 \cos(\omega_2 t)dt, \tag{39}$$

the Hamiltonian-based nonlinear frequency is obtained as [48]:

$$\omega_{HFAF}^2 = \frac{\omega_2^2\bar{R}_1 - \omega_1^2\bar{R}_2}{\bar{R}_1 - \bar{R}_2}, \tag{40}$$

where ω_1 and ω_2 are typically chosen as $\omega_1 = 1$ and $\omega_2 = 2$. The Hamiltonian formulation of the present problem is expressed as

$$H = \frac{1}{2}\left(\frac{du}{dt}\right)^2 + \frac{1}{2}\beta_1\left(\frac{du}{dt}\right)^2 u^2 + \frac{1}{2}\beta_2 u^2 + \frac{1}{4}\beta_3 u^4 + \frac{1}{6}\beta_4 u^6. \tag{41}$$

Considering the initial conditions given in Eq. (12) and applying Eq. (37), the residual function is constructed as follows:

$$\begin{aligned} R(t) = {} & \frac{1}{2}\left(-A\omega\sin(\omega t)\right)^2 + \frac{1}{2}\beta_1 A^2\left(-A\omega\sin(\omega t)\right)^2\cos^2(\omega t) + \frac{1}{2}\beta_2 A^2\left(\cos^2(\omega t) - 1\right) \\ & + \frac{1}{4}\beta_3 A^4\left(\cos^4(\omega t) - 1\right) + \frac{1}{6}\beta_4 A^6\left(\cos^6(\omega t) - 1\right). \end{aligned} \tag{42}$$

Assuming $\omega_1 = 1$ and $\omega_2 = 2$, the corresponding average residuals are obtained as follows:

$$\bar{R}_1 = \frac{2}{15\pi}\beta_1 A^4 - \frac{1}{3\pi}\beta_2 A^2 - \frac{7}{30\pi}\beta_3 A^4 - \frac{19}{105\pi}\beta_4 A^6 + \frac{1}{3\pi}A^2. \tag{43}$$

$$\bar{R}_2 = \frac{8}{15\pi}\beta_1 A^4 - \frac{1}{3\pi}\beta_2 A^2 - \frac{7}{30\pi}\beta_3 A^4 - \frac{19}{105\pi}\beta_4 A^6 + \frac{4}{3\pi}A^2. \tag{44}$$

Following Eq. (40), the Hamiltonian-based expression for the nonlinear frequency of the stringer-stiffened shell is obtained as:

$$\omega_{HFAF} = \sqrt{\frac{70\beta_2 + 49\beta_3 A^2 + 38\beta_4 A^4}{70 + 28\beta_1 A^2}}, \tag{45}$$

and the approximate solution as:

$$u_{HFAF}(t) = A\cos\left(\sqrt{\frac{70\beta_2 + 49\beta_3 A^2 + 38\beta_4 A^4}{70 + 28\beta_1 A^2}}t\right). \tag{46}$$

This method performs well at large amplitudes due to its foundation in energy principles. Its energy-based formulation enables more accurate capture of nonlinear effects within this range.

3.4. Exact Nonlinear Frequency

To obtain the exact nonlinear frequency of the stringer-stiffened shell, the Hamiltonian form derived in Eq. (41) is employed. Using the initial conditions given in Eq. (12), and considering that the Hamiltonian remains constant in a conservative system, the following relation is obtained:

$$\frac{1}{2}\left(\frac{du}{dt}\right)^2 + \frac{1}{2}\beta_1\left(\frac{du}{dt}\right)^2 u^2 + \frac{1}{2}\beta_2 u^2 + \frac{1}{4}\beta_3 u^4 + \frac{1}{6}\beta_4 u^6 = \frac{1}{2}\beta_2 A^2 + \frac{1}{4}\beta_3 A^4 + \frac{1}{6}\beta_4 A^6. \tag{47}$$

Eq. (47) can be rewritten as follows:

$$\left(\frac{du}{dt}\right)^2 = \frac{\beta_2\left(A^2 - u^2\right) + \frac{1}{2}\beta_3\left(A^4 - u^4\right) + \frac{1}{3}\beta_4\left(A^6 - u^6\right)}{1 + \beta_1 u^2}. \tag{48}$$

Solving Eq. (48) for dt, we obtain:

$$dt = \pm\sqrt{\frac{1 + \beta_1 u^2}{\beta_2\left(A^2 - u^2\right) + \frac{1}{2}\beta_3\left(A^4 - u^4\right) + \frac{1}{3}\beta_4\left(A^6 - u^6\right)}}du. \tag{49}$$

Since the period of the oscillator is four times the duration required to move from 0 to A, we have

$$T_{exact} = 4\int_0^A \sqrt{\frac{1+\beta_1 u^2}{\beta_2\left(A^2-u^2\right)+\frac{1}{2}\beta_3\left(A^4-u^4\right)+\frac{1}{3}\beta_4\left(A^6-u^6\right)}}du. \tag{50}$$

Therefore, the exact nonlinear frequency of the stringer-stiffened shell is obtained as follows:

$$\omega_{exact} = \frac{2\pi}{4\int_0^A \sqrt{\frac{1+\beta_1 u^2}{\beta_2\left(A^2-u^2\right)+\frac{1}{2}\beta_3\left(A^4-u^4\right)+\frac{1}{3}\beta_4\left(A^6-u^6\right)}}du}. \tag{51}$$

This integral typically requires numerical evaluation or the use of elliptic functions, serving as a benchmark for approximate methods.

4. Results and Discussion

This section evaluates the nonlinear frequencies of a stringer-stiffened cylindrical shell using the proposed methods. The results are presented for SS BCs and are validated through comparisons with both exact and numerical solutions. Tables 1-3 report the nonlinear frequencies and relative errors for non-dimensional amplitudes A ranging from 0.01 to 3. The parameter sets are as follows: Table 1 (case1: $\beta_1 = 0.5$, $\beta_2 = 2$, $\beta_3 = 0.2$, $\beta_4 = 0.1$); Table 2 (case 2: $\beta_1 = 0.1$, $\beta_2 = 1$, $\beta_3 = 0.5$, $\beta_4 = 0.2$); and Table 3 (case 3: $\beta_1 = 0.9$, $\beta_2 = 1.5$, $\beta_3 = 2.5$, $\beta_4 = 3.5$), reflecting increasing degrees of nonlinearity. The results are compared with the exact solutions and with those reported in [40] using the HPM. To facilitate clearer comparison, the relative errors reported in Tables 1-3 are also illustrated in Fig. 2 as a function of amplitude. It can be observed that for small amplitudes ($A \leq 0.2$), all methods exhibit high accuracy, with errors below 0.1% across all parameter sets. This behavior is expected, as the cubic and quintic terms in Eq. (8) contribute minimally at low A, making the system nearly linear. The results of ALPF and SEMF methods are identical to the exact solution for $A \leq 0.1$, while the Hamiltonian-based method shows slight deviations (e.g., 0.09% error at $A = 0.2$ in Table 1), likely due to its sensitivity to higher-order nonlinear terms. At large amplitudes ($A \geq 1$), the errors increase, particularly for He's method, which reaches 10.26% at $A = 3$ in Table 3. In contrast, the ALPF and SEMF show improved performance, with errors up to 5.89% at $A = 3$, benefiting from their error minimization strategies. The Hamiltonian method consistently outperforms the others, maintaining errors below 3.92% at $A = 3$, as its energy-based framework more effectively captures the nonlinear dynamic behavior. It is noteworthy that both the ALPF and SEMF methods accurately predict the frequencies obtained by the HPM, while offering a simpler computational procedure. Furthermore, the computational time required to evaluate the frequency using the proposed methods is minimal, demonstrating their high efficiency. For instance, for the case of $A = 3$ in Table 1, the computation times on a system with an Intel Core i7-7500U CPU and 12 GB RAM, using MATLAB, are approximately 0.1 ms, 0.03 ms, and 0.006 ms for the ALPF, SEME, and HFAF methods, respectively. In comparison, the exact method requires about 1.3 ms due to the necessity for numerical integration.

Table 1 Comparison of the frequencies obtained by the proposed three methods with exact ones for $\beta_1 = 0.5$, $\beta_2 = 2$, $\beta_3 = 0.2$, $\beta_4 = 0.1$.

A	*present*					ω_{HPM} [38]
	ω_{exact}	ω_{He}	ω_{ALPF}	ω_{SEMF}	ω_{HFAF}	
0.01	1.4142	1.4142	1.4142	1.4142	1.4142	1.4142
0.1	1.4130	1.4130	1.4130	1.4130	1.4133	1.4130
0.2	1.4093	1.4093	1.4093	1.4093	1.4106	1.4093
0.8	1.3544	1.3516	1.3524	1.3524	1.3683	1.3524
1	1.3347	1.3285	1.3304	1.3304	1.3522	1.3304
1.4	1.3162	1.2979	1.3041	1.3041	1.3356	1.3041
1.8	1.3411	1.3037	1.3176	1.3176	1.3545	1.3176
2	1.3719	1.3229	1.3416	1.3416	1.3801	1.3416
2.5	1.4985	1.4156	1.4488	1.4488	1.4900	1.4488
3	1.6820	1.5597	1.6089	1.6089	1.6537	1.6089

Table 2 Comparison of the frequencies obtained by the proposed three methods with exact ones for $\beta_1 = 0.1$, $\beta_2 = 1$, $\beta_3 = 0.5$, $\beta_4 = 0.2$.

A	*present*					ω_{HPM} [38]
	ω_{exact}	ω_{He}	ω_{ALPF}	ω_{SEMF}	ω_{HFAF}	
0.01	1.0000	1.0000	1.0000	1.0000	1.0000	1.0000
0.1	1.0016	1.0016	1.0016	1.0016	1.0016	1.0016
0.2	1.0066	1.0066	1.0066	1.0066	1.0063	1.0066
0.8	1.1175	1.1163	1.1186	1.1186	1.1121	1.1186
1	1.1926	1.1902	1.1952	1.1952	1.1843	1.1952
1.4	1.4110	1.4049	1.4204	1.4204	1.3965	1.4204
1.8	1.7215	1.7095	1.7423	1.7423	1.7024	1.7423
2	1.9093	1.8930	1.9365	1.9365	1.8885	1.9365
2.5	2.4621	2.4281	2.5036	2.5036	2.4378	2.5036
3	3.1145	3.0499	3.1623	3.1623	3.0851	3.1623

Table 3 Comparison of the frequencies obtained by the proposed three methods with exact ones for $\beta_1 = 0.9$, $\beta_2 = 1.5$, $\beta_3 = 2.5$, $\beta_4 = 3.5$.

A	*present*					ω_{HPM} [38]
	ω_{exact}	ω_{He}	ω_{ALPF}	ω_{SEMF}	ω_{HFAF}	
0.01	1.2248	1.2248	1.2248	1.2248	1.2248	1.2248
0.1	1.2297	1.2297	1.2297	1.2297	1.2297	1.2297
0.2	1.2452	1.2451	1.2452	1.2452	1.2453	1.2452
0.8	1.6689	1.6500	1.6709	1.6709	1.6619	1.6709
1	1.9571	1.9197	1.9586	1.9586	1.9460	1.9586
1.4	2.7040	2.6016	2.6861	2.6861	2.6777	2.6861
1.8	3.5965	3.3897	3.5248	3.5248	3.5378	3.5248
2	4.0750	3.8032	3.9641	3.9641	3.9928	3.9641
2.5	5.3237	4.8620	5.0873	5.0873	5.1637	5.0873
3	6.6127	5.9344	6.2230	6.2230	6.3534	6.2230

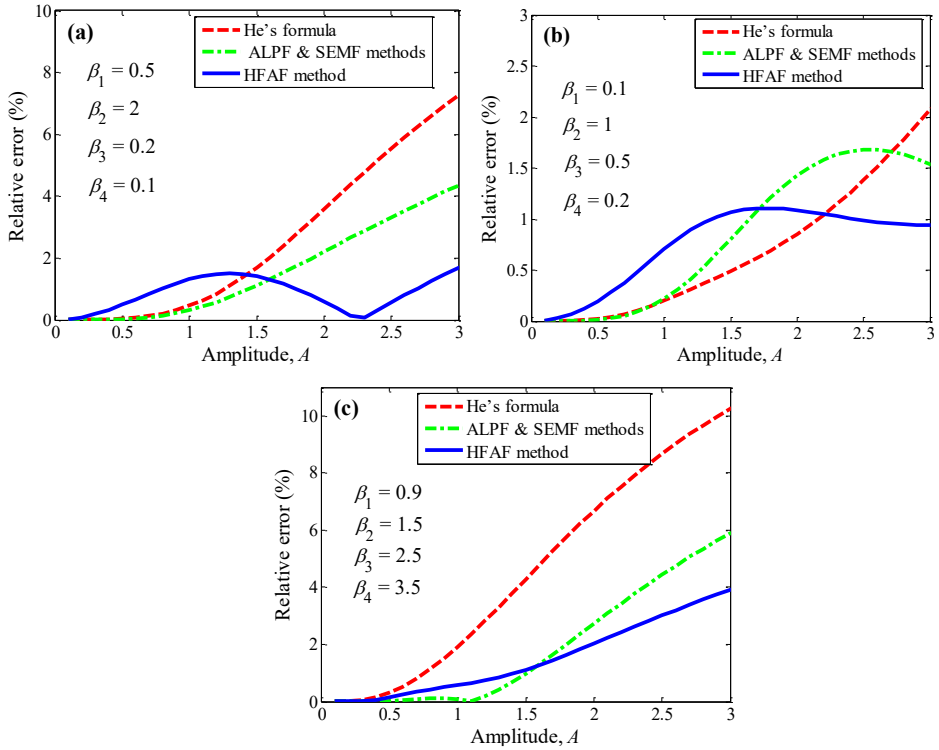

Fig. 2 The relative error with respect to amplitude for the three proposed methods under various system parameters, (a) case 1, (b) case 2, and (c) case 3

Fig. 3 illustrates the periodic solutions obtained by the proposed methods in comparison with the numerical solution. All methods demonstrate acceptable accuracy and successfully capture the periodic behavior of the stringer-stiffened shell. Compared to previous studies, the proposed methods offer simpler alternatives to iterative approaches such as HPM [38] and GRHBM [39], which involve complex series expansions and exhibit limitations at large amplitude values. Accurate frequency prediction is essential for avoiding resonance in stiffened shells, thereby enhancing safety in applications such as aircraft and submarines. He's method, due to its simplicity and errors below 2% for $A \leq 1$, is particularly suitable for rapid design iterations during preliminary engineering analyses. The Hamiltonian-based method, with errors remaining below 4% for all amplitude levels, is better suited for critical applications that demand high precision, such as spacecraft panels subjected to large dynamic loads. These methods enable engineers to optimize shell designs more efficiently, reducing costs and improving structural integrity.

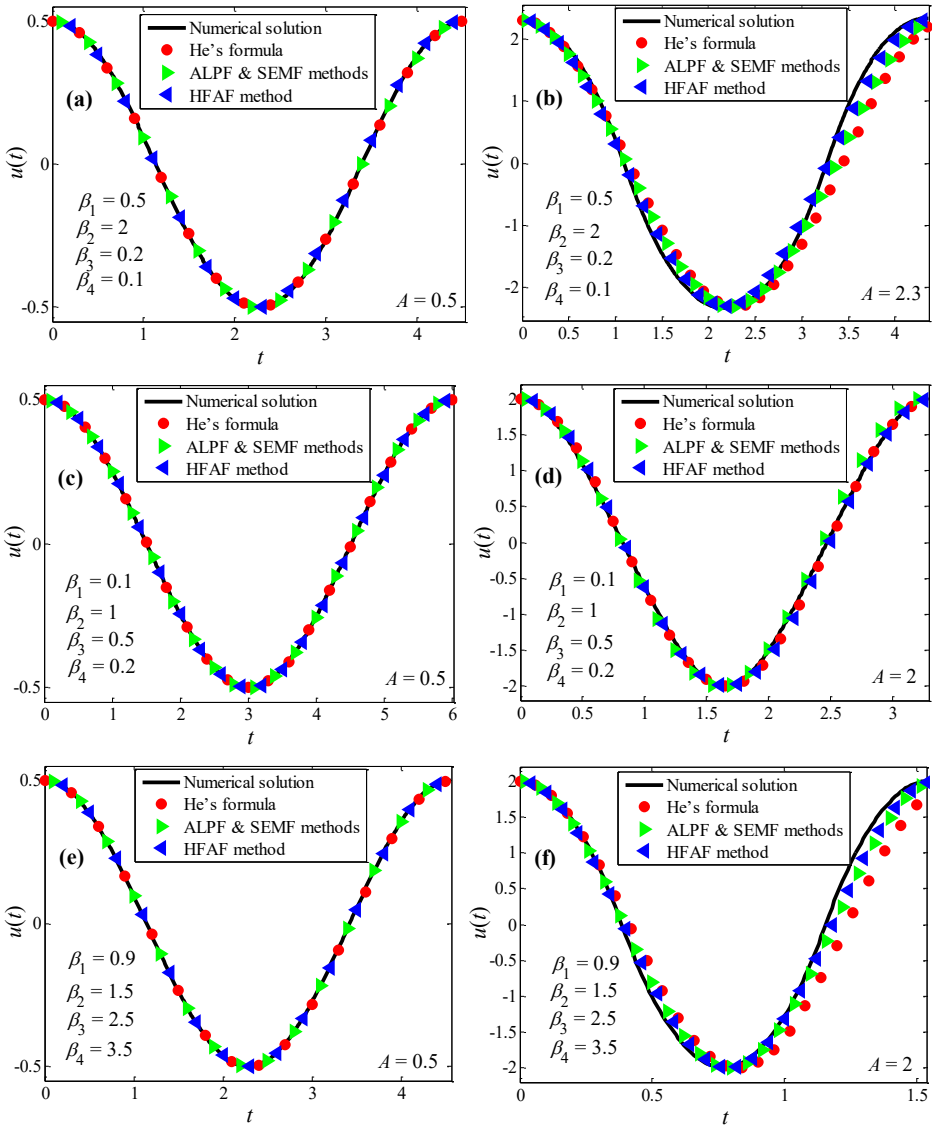

Fig. 3 Comparison of the analytical solutions with the numerical solution for various system parameters and amplitudes, (a) case 1, $A = 0.5$, (b) case 1, $A = 2.3$, (c) case 2, A=0.5, (d) case 2, $A = 2$, (e) case 3, $A = 0.5$, and (f) case 3, $A = 2$

Using the frequency-amplitude relationship derived from the Hamiltonian-based frequency-amplitude method, Fig. 4 illustrates the variation of the frequency ratio (ω_{NL}/ω_L) with respect to amplitude under various system parameters. In this figure, when the effect of one parameter is studied, the other three parameters are fixed at unity. It is observed that parameters β_1 and β_2 have a similar effect. As their values increase, the frequency ratio

decreases. In contrast, parameters β_3 and β_4 exhibit the opposite trend. An increase in these parameters results in an increase in the nonlinear to linear frequency ratio.

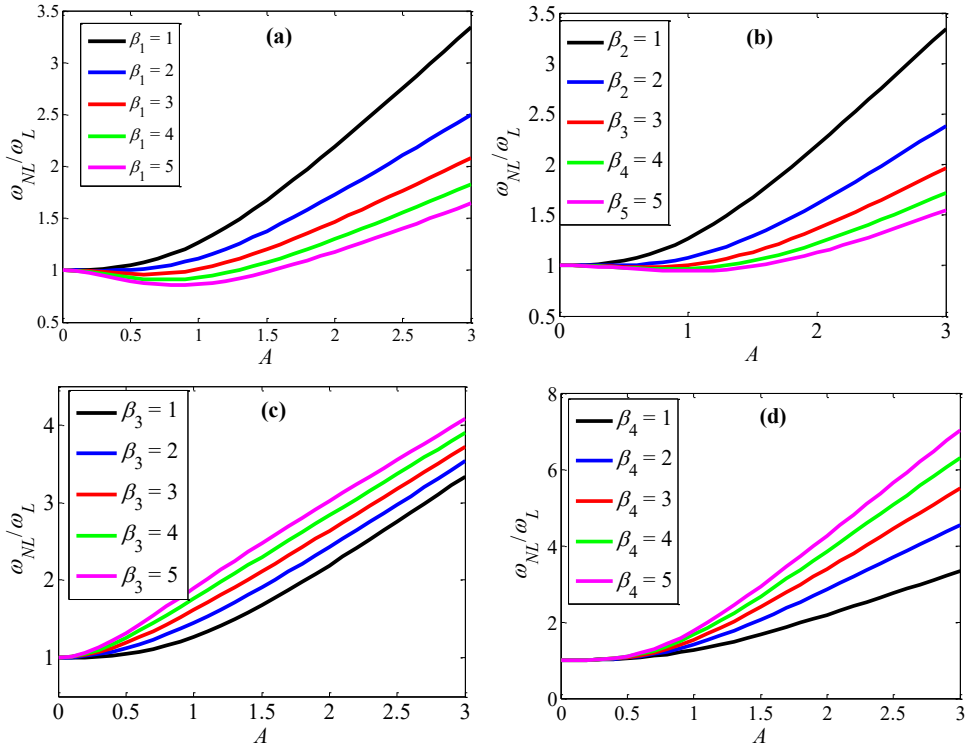

Fig. 4 The effect of system parameters (a) β_1, (b) β_2, (c) β_3, and (d) β_4 on the variation of frequency ratio with respect to the amplitude

Fig. 5 presents a sensitivity analysis of the frequency ratio with respect to various system parameters under different amplitudes. As expected, at small amplitudes (here A = 0.1), the frequency ratio is equal to unity, indicating the negligible effect of nonlinear terms. Figs. 5a and 5b show that, for various amplitudes, an increase in the parameters β_1 and β_2 results in the frequency ratio approaching unity, thereby reducing the impact of nonlinearities. Specifically, Fig. 5a indicates that for moderate amplitudes (here A = 0.5 and A = 1.5), the frequency ratio may be either greater or less than unity, depending on the value of β_1. For instance, at A = 1.5, the frequency ratio is approximately 1.2 when β_1 = 2, while it decreases to nearly 0.9 when β_1 = 5. However, at higher amplitudes, the ratio exceeds for all values of β_1. It is important to note that, as defined in Eq. (8), the parameter β_1 quantifies the contribution of displacement-dependent terms. Therefore, it may be concluded that the influence of these terms on the nonlinear frequency of stringer-stiffened shell becomes significant at larger amplitudes. Furthermore, Figs. 5c and 5d reveal that the frequency ratio increases with higher values of β_3 and β_4, indicating the role of cubic-quintic nonlinearities in the nonlinear frequency response of the structure.

Using the expressions derived for the nonlinear frequency of the stringer-stiffened shell, the influence of geometric parameters can be readily examined. For instance, Fig. 6 illustrates the effects of the number of stringers N and the amplitude A on the nonlinear frequency under both SS and CC BCs. The geometrical and material properties of the shell are as follows [49]: radius $R = 242$ mm, thickness $h = 0.65$ mm, length $L = 609$ mm, Elastic modulus $E = 68.95$ Gpa, Poisson's ratio $v = 0.3$, and density $\rho = 2714$ kg/m^3. The depth and width of the stringers are taken as 7.02 mm and 2.55 mm, respectively, with the assumption that the shell and stringers are made of the same materials. As shown in Fig. 6, increasing the number of stringers leads to a higher nonlinear frequency due to the corresponding increase in structural stiffness. Additionally, as the amplitude increases, the frequency initially decreases and then increases. This initial drop in frequency persists up to higher amplitude levels for CC BCs compared to SS ones. Fig. 7 further demonstrates that the nonlinear frequency increases with increasing shell thickness h. Similarly, the effects of other geometric parameters can be systematically explored using the derived expressions.

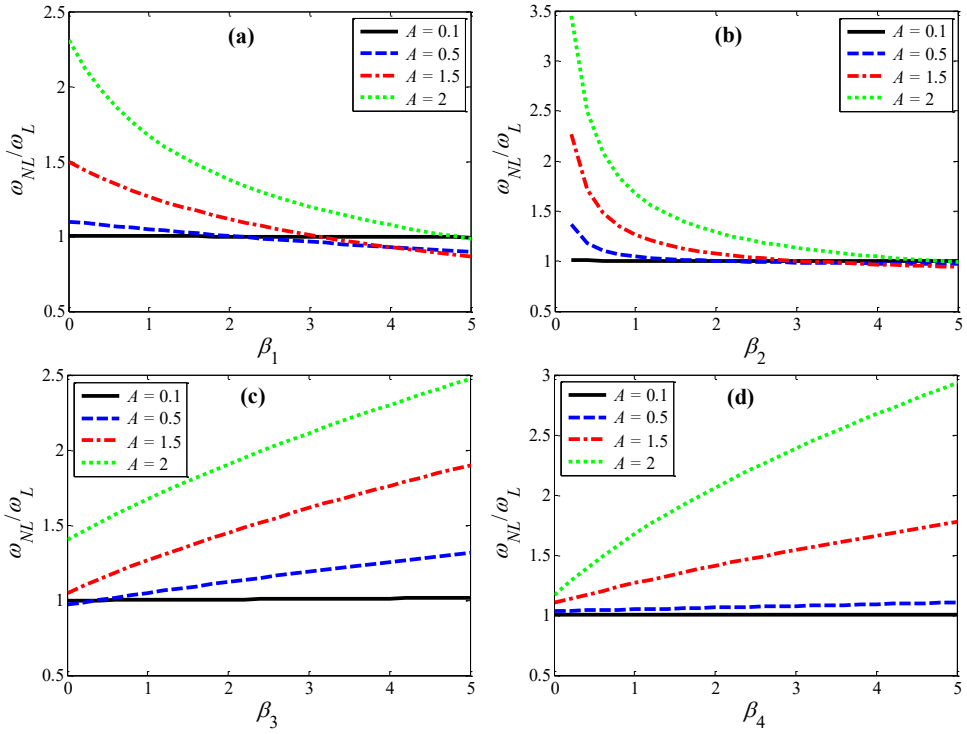

Fig. 5 The variation of frequency ratio with respect to (a) β_1, (b) β_2, (c) β_3, and (d) β_4 under various amplitudes

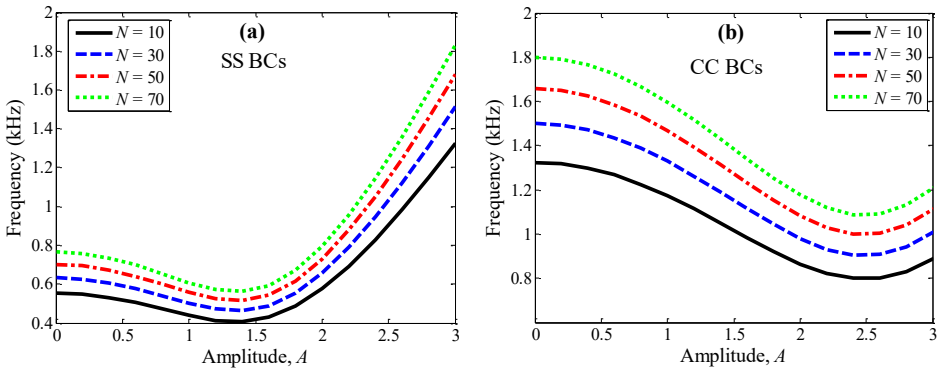

Fig. 6 The effects of the number of stringers N and amplitude A on the frequency of a stringer-stiffened shell when $m = n = 1$. (a) SS BCs, (b) CC BCs

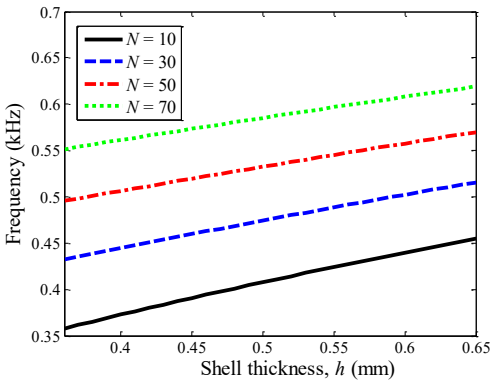

Fig. 7 The effects of the number of stringers N and shell thickness h on the frequency of a stringer-stiffened shell under SS BCs. $m = n = 1$

5. CONCLUSION

This study developed three analytical methods: adaptive location point-based He's formulation (ALPF), square error minimizing-based frequency formulation (SEMF), and Hamiltonian-based frequency-amplitude formulation (HFAF), to derive closed-form expressions for the nonlinear frequency of stringer-stiffened cylindrical shells. These methods were validated against both exact and numerical solutions. For small vibration amplitudes, they exhibited errors les than 0.1%, while for larger amplitudes, the Hamiltonian-based method maintained an error within to 3.92%. Compared to iterative techniques such as the homotopy perturbation method, the proposed methods offer efficiency and ease of application. The models effectively address the cubic-quintic nonlinearities characteristic of stiffened shells, offering practical tools for fast and accurate frequency prediction. These findings are particularly relevant to aerospace structures, spacecraft panels, and marine hulls, where avoiding resonance is essential for ensuring structural safety.

It is important to note that the present study focused on the vibration response in a single dominant mode and neglected damping effects. These assumptions were adopted to facilitate the development of simple, fast, and non-iterative analytical expressions for the

nonlinear frequency of stringer-stiffened shells. While this approach effectively captures the primary nonlinear behavior, it does not account for potential multi-mode interactions or energy dissipation mechanisms, which may influence the dynamic response in more complex scenarios. These limitations suggest valuable directions for future research, including the extension of the proposed methods to multi-mode systems and the incorporation of damping effects for a more comprehensive dynamic analysis.

REFERENCES

1. Gavrilenko, G.D., Matsner, V.I., 2006, *Some features of the buckling of stringer shells*, International Applied Mechanics, 42(2), pp. 176-180.
2. Naghsh, A., Saadatpour, M.M., Azhari, M., 2015, *Free vibration analysis of stringer stiffened general shells of revolution using a meridional finite strip method*, Thin-Walled Structures, 94, pp. 651-662.
3. Golchi, M., Mostafa, T., Talebitooti, R., 2019, *Thermal buckling and free vibration of FG truncated conical shells with stringer and ring stiffeners using differential quadrature method*, Mechanics Based Design of Structures and Machines, 47(3), pp. 255-282.
4. Bich, D.H., Ninh, D.G., 2017, *An analytical approach: Nonlinear vibration of imperfect stiffened FGM sandwich toroidal shell segments containing fluid under external thermo-mechanical loads*, Composite Structures, 162, pp. 164-181.
5. Ninh, D.G., Bich, D.H., 2016, *Nonlinear thermal vibration of eccentrically stiffened Ceramic-FGM-Metal layer toroidal shell segments surrounded by elastic foundation*, Thin-Walled Structures, 104, pp. 198-210.
6. Liu, L., Sun, S., Han, J., 2021, *Nonlinear traveling-wave vibration of a ring-stringer stiffened cylindrical shell*, International Journal of Structural Stability and Dynamics, 21(04), 2150059.
7. Liu, Y., Qin, Z., Chu, F., 2022, *Nonlinear forced vibrations of rotating cylindrical shells under multi-harmonic excitations in thermal environment*, Nonlinear Dynamics, 108(4), pp. 2977-2991.
8. Vahidi, H., Shahgholi, M., Hanzaki, A.R., Mohamadi, A., 2022, *Nonlinear vibration, stability, and bifurcation of rotating axially moving conical shells*, Acta Mechanica, 233(8), pp. 3175-3196.
9. Mohammadrezazadeh, S., Jafari, A.A., 2023, *Nonlinear vibration suppression of S-S and C-C laminated composite cylindrical shells with magnetostrictive strips*, Mechanics Based Design of Structures and Machines, 51(10), pp. 5470-5491.
10. Bochkarev, S.A., Lekomtsev, S.V., Matveenko, V.P., 2023, *Finite element analysis of the panel flutter of stiffened shallow shells*, Continuum Mechanics and Thermodynamics, 35(4), pp. 1275-1290.
11. Foroutan, K., Dai, L., 2024, *Nonlinear dynamic response and vibration of spiral stiffened FG toroidal shell segments with variable thickness*, Mechanics Based Design of Structures and Machines, 52(8), pp. 4930-4952.
12. Azzara, R., Filippi, M., Carrera, E., 2024, *Rotordynamic analyses of stiffened cylindrical structures using high-fidelity shell models*, Mechanics of Advanced Materials and Structures, 31(29), pp. 11677-11686.
13. Zhang, J., Zhang, W., Zhang, Y.F., 2024, *Nonlinear vibrations of porous-hyperelastic cylindrical shell under harmonic force using harmonic balance and pseudo-arc length continuation methods*, Thin-Walled Structures, 198, 111767.
14. Du, Y., Tang, Y., Zou, Y., Wang, Y., Pang, F., Jia, F., Ma, Y., Wang, S., 2024, *The low frequency multi-linear spectrum vibration control study of cylindrical shell through a semi-analytical method*, Thin-Walled Structures, 196, 111521.
15. Chen, Z., Liu, H., Ma, L., Gan, J., Wu, W., 2025, *Investigation on the correlation between welding parameters and vibro-acoustic characteristics in the stiffened cylindrical shells*, Ocean Engineering, 321, 120355.
16. Tan, N.C., Dzung, N.M., Ha, N.H., Tien, N.D., Hung, N.C., Sofiyev, A.H., Ninh, D.G., 2025, *Novel sandwich composite shell structures in nonlinear geometric and dynamic analyses*, AIAA Journal, https://doi.org/10.2514/1.J065315.
17. Khoddami Maraghi, Z., Safari, I., Ghorbanpour Arani, A., Shekari, A.M., Saeidnejad, S., Zahedi Bidgoli, A., 2025, *Free vibration analysis of sandwich graphene-reinforced nanocomposite truncated conical shells with auxetic honeycomb core*, The Journal of Strain Analysis for Engineering Design, https://doi.org/10.1177/03093247241311390.
18. Jiang, J., Olson, M.D., 1994, *Vibration analysis of orthogonally stiffened cylindrical shells using super finite elements*, Journal of Sound and Vibration, 173(1), pp. 73-83.
19. Stanley, A.J., Ganesan, N., 1997, *Free vibration characteristics of stiffened cylindrical shells*, Computers & Structures, 65(1), pp. 33-45.
20. Rama, G., Marinković, D., Zehn, M., 2018, *Efficient three-node finite shell element for linear and geometrically nonlinear analyses of piezoelectric laminated structures*, Journal of Intelligent Material Systems and Structures, 29(3), pp. 345-357.

21. Milić, P., Marinković, D., Klinge, S., Ćojbašić, Ž., 2023, *Reissner-Mindlin based isogeometric finite element formulation for piezoelectric active laminated shells*, Tehnički Vjesnik, 30(2), pp. 416-425.
22. Mohammadian, M., Ismail, G.M., 2024, *Improved harmonic balance method for analyzing asymmetric restoring force functions in nonlinear vibration of mechanical systems*, Physica Scripta, 99(7), 075280.
23. Chen, Y., Hou, L., Lin, R., Toh, W., Ng, T., Chen, Y., 2024, *A general and efficient harmonic balance method for nonlinear dynamic simulation*, International Journal of Mechanical Sciences, 276, 109388.
24. Fu, Y., Zhang, J., Wan, L., 2011, *Application of the energy balance method to a nonlinear oscillator arising in the microelectromechanical system (MEMS)*, Current Applied Physics, 11(3), pp. 482-485.
25. Molla, M.H.U., Alam, M.S., 2017, *Higher accuracy analytical approximations to nonlinear oscillators with discontinuity by energy balance method*, Results in Physics, 7, pp. 2104-2110.
26. He, J.-H., 2003, *Homotopy perturbation method: a new nonlinear analytical technique*, Applied Mathematics and Computation, 135(1), pp. 73-79.
27. Mohammadian, M., 2024, *Application of He's new frequency-amplitude formulation for the nonlinear oscillators by introducing a new trend for determining the location points*, Chinese Journal of Physics, 89, pp. 1024-1040.
28. He, J.-H., 2010, *Hamiltonian approach to nonlinear oscillators*, Physics Letters A, 374(23), pp. 2312-2314.
29. Akter, R., 2024, *Soliton dynamics and multistability analysis of the Hamiltonian amplitude model*, Results in Physics, 63, 107878.
30. Mohammadian, M., 2017, *Application of the variational iteration method to nonlinear vibrations of nanobeams induced by the van der Waals force under different boundary conditions*, The European Physical Journal Plus, 132(4), 169.
31. Ahmad, H., Ozsahin, D.U., Farooq, U., Fahmy, M.A., Albalwi, M.D., Abu-Zinadah, H., 2023, *Comparative analysis of new approximate analytical method and Mohand variational transform method for the solution of wave-like equations with variable coefficients*, Results in Physics, 51, 106623.
32. Farzaneh, Y., Akbarzadeh Tootoonchi, A., 2010, *Global mrror minimization method for solving strongly nonlinear oscillator differential equations*, Computers & Mathematics with Applications, 59(8), pp. 2887-2895.
33. Ismail, G.M., Abu-Zinadah, H., 2021, *Analytic approximations to non-linear third order jerk equations via modified global error minimization method*, Journal of King Saud University - Science, 33(1), 101219.
34. Mohammadian, M., Shariati, M., 2020, *Application of AG method and its improvement to nonlinear damped oscillators*, Scientia Iranica, 27(1), pp. 203-214.
35. Mohammadian, M., 2021, *Approximate analytical solutions to nonlinear damped oscillatory systems using a modified algebraic method*, Journal of Applied Mechanics and Technical Physics, 62(1), pp. 70-78.
36. He, J.-H., 2007, *Variational approach for nonlinear oscillators*, Chaos, Solitons & Fractals, 34(5), pp. 1430-1439.
37. Bayat, M., Pakar, I., Cveticanin, L., 2014, *Nonlinear vibration of stringer shell by means of extended Hamiltonian approach*, Archive of Applied Mechanics, 84(1), pp. 43-50.
38. Pakar, I., Bayat, M., 2015, *Nonlinear vibration of stringer shell: An analytical approach*, Proceedings of the Institution of Mechanical Engineers, Part E: Journal of Process Mechanical Engineering, 229(1), pp. 44-51.
39. Farea, N.M., Ismail, G.M., 2025, *Analytical solution for strongly nonlinear vibration of a stringer shell*, Journal of Low Frequency Noise, Vibration and Active Control, 44(1), pp. 81-87.
40. Evkin, A.Y., Kalamkarov, A.L., 2001, *Analysis of large deflection equilibrium states of composite shells of revolution. Part 1. General model and singular perturbation analysis*, International journal of solids and structures, 38(50-51), pp. 8961-8974.
41. Awrejcewicz, J., Andrianov, I.V., Manevitch, L.I., 2012, *Asymptotic Approaches in Nonlinear Dynamics: New Trends and Applications*, Springer Science & Business Media, Berlin.
42. Bayat, M., Pakar, I., Bayat, M., 2011. *Analytical study on the vibration frequencies of tapered beams,* Latin American Journal of Solids and Structures, 8, pp. 149-162.
43. Mohammadian, M., 2021, *Nonlinear free vibration of damped and undamped bi-directional functionally graded beams using a cubic-quintic nonlinear model*, Composite Structures, 255, 112866.
44. He, J.-H., 2025, *Frequency-amplitude relationship in nonlinear oscillators with irrational nonlinearities*, Spectrum of Mechanical Engineering and Operational Research, 2(1), pp. 121-129.
45. He, J.-H., 2019, *The simpler, the better: Analytical methods for nonlinear oscillators and fractional oscillators*, Journal of Low Frequency Noise, Vibration and Active Control, 38(3-4), pp. 1252-1260.
46. Zhang, Y., Tian, D., Pang, J., 2022, *A fast estimation of the frequency property of the microelectromechanical system oscillator*, Journal of Low Frequency Noise, Vibration and Active Control, 41(1), pp. 160-166.
47. He, C.-H., Liu, C., 2022, *A modified frequency–amplitude formulation for fractal vibration systems*, Fractals, 30(03), 2250046.
48. Wang, K.-J., Wang, G.-D., 2021, *Study on the nonlinear vibration of embedded carbon nanotube via the Hamiltonian-based method*, Journal of Low Frequency Noise, Vibration and Active Control, 41(1), pp. 112-117.
49. Zhao, X., Liew, K.M., Ng, T.Y., 2002, *Vibrations of rotating cross-ply laminated circular cylindrical shells with stringer and ring stiffeners*, International Journal of Solids and Structures, 39, pp. 529-545.